ONLINE DETECTION OF SCALP-INVISIBLE MESIAL-TEMPORAL BRAIN INTERICTAL EPILEPTIFORM DISCHARGES FROM EEG

Bahman Abdi-Sargezeh[*], *Antonio Valentin*[†], *Gonzalo Alarcon*[‡], *and Saeid Sanei* [*]

[*]School of Science and Technology, Nottingham Trent University, UK
[†] Department of Clinical Neuroscience, King's College London, UK
[‡] Department of Neurology, Hamad General Hospital, Doha, Qatar

ABSTRACT

Brain interictal epileptiform discharges (IEDs) are transient events occurring between two or before seizure onsets. The IEDs are captured mainly by the intracranial EEG (iEEG) and only 4.7% of them are visible in our scalp EEG (sEEG) dataset. Here, we propose a method namely temporal components analysis (TCA) to detect the IEDs from ongoing sEEG and iEEG signals recorded simultaneously. In addition, spatial components analysis (SCA) previously proposed by ourselves is employed to detect the IEDs. Finally, both TCA and SCA are combined to boost the IED detection system performance. This method is referred as to TCA-SCA. The proposed TCA-SCA method detects the IEDs from the iEEG and sEEG by 81.2% and 37.4% sensitivity, respectively. The findings show that our proposed method enables the detection of scalp-invisible IEDs from ongoing sEEG recordings.

Index Terms— EEG, interictal epileptiform discharges, IED detection, tensor decomposition.

1. INTRODUCTION

Epilepsy is a chronic brain disease characterized by epileptic seizures occurring due to excessive discharges of a group (or groups) of neurons in the cerebral cortex or hippocampus. Some transient activities called interictal epileptiform discharges (IEDs) occur between two or before seizure onsets. The IED signatures are captured using electroencephalogram (EEG), and their detection can help to manage and monitor epilepsy [1].

Foramen ovale (FO) electrodes are used for recording intracranial EEG (iEEG) signals from the brain mesial temporal lope [2]. FO electrodes are introduced bilaterally through the FO anatomical holes into ambient cistern and placed on the exposed mesial temporal structures [3, 4]. Therefore, they provide an opportunity to simultaneous record the scalp EEG (sEEG) and iEEG without disruption to brain coverings [5]. However, studies conducted on simultaneously sEEG and iEEG recordings have shown that a small percentage of IED, 9% in [6] and 22% in [7], is observable over the scalp. Therefore, developing a method to detect scalp-invisible IEDs from the sEEG is of paramount importance since the sEEG is recorded by non-invasive methods.

Different techniques and algorithms, including time-frequency (TF) representation [8] and deep learning [9, 10], have been used for IED detection. However, tensor factorization approach has been very successful in exploiting the waveform structure in various domains, segments, and subjects [11–14]. It provides an opportunity to consider the data diversity. This means that different aspects of data (e.g. time, frequency, space, trial, and subject) can be analyzed together by tensor factorization. We already developed a tensor-based method to detect the IEDs from sEEG signals by concatenating the IED segments into a three-way tensor with the dimension of time, channel, and segment [15]. Spyrou *et al.* detected the IEDs by analyzing time, frequency, space, and segment domains together by tensor factorization [12].

The main drawback for these methods is that the IED positions are aligned in all the segments. Whereas, in real world, the aim is to detect the IEDs from ongoing EEG recordings in which there is no alignment among the IED segments. In this study, we aim to detect the IEDs from ongoing sEEG and iEEG signals. To do so, we first develop a tensor-based method, namely temporal component analysis (TCA). In addition, our already developed method, called spatial component analysis (SCA), is employed to this end. Finally, both SCA and TCA are combined, referred to as TCA-SCA, to improve the performance.

2. METHODS

In terms of morphology and IED source locations, the IEDs are similar. Therefore, they may share some features. In contrast, normal brain activities or artifacts are entirely independent from these discharges. As a result, in our methods, all IEDs are concatenated into a three-way tensor with the dimension of time, channel, and IED segment. Then, the tensor is decomposed to temporal, spatial, and segmental factors by employing CANDECOMP/PARAFAC decomposition (CPD) [16]. Finally, both IED and non-IED segments are projected onto the temporal factors in TCA, and onto the spatial

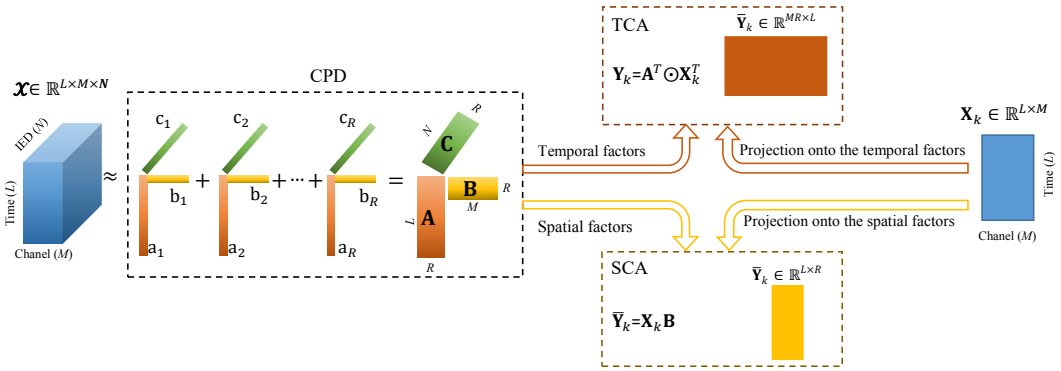

Fig. 1: The proposed IED detection models. $\boldsymbol{\mathcal{X}}$ includes the IED segments only. CPD is applied to $\boldsymbol{\mathcal{X}}$ to decompose it to temporal, spatial, and segmental factors. $\mathbf{X}_k$ is an IED or non-IED segment from the training or test data, which is projected onto the temporal factors $\mathbf{A}$ in TCA and onto the spatial factors $\mathbf{B}$ in SCA.

factors in SCA. It should be noted that the idea of concatenating only IEDs into a tensor was already used and provided appropriate results [14, 15].

Suppose our training dataset consists of N IED segments with L time samples and M channels. All IEDs are concatenated into a tensor $\boldsymbol{\mathcal{X}} \in \mathbb{R}^{L\times M\times N}$. CPD is employed to factorize the tensor into a sum of rank-one tensors as follows:

$$\boldsymbol{\mathcal{X}} \approx \sum_{r=1}^{R} \mathbf{a}_r \circ \mathbf{b}_r \circ \mathbf{c}_r, \tag{1}$$

where the symbol '$\circ$' indicates vector outer product, R is a positive integer, and $\mathbf{a}_r \in \mathbb{R}^L, \mathbf{b}_r \in \mathbb{R}^M, \mathbf{c}_r \in \mathbb{R}^N$ for $r = 1, \ldots, R$. The factor matrices are constructed from the combination of vectors from the rank-one components, i.e., $\mathbf{A} = [\mathbf{a}_1 \ldots \mathbf{a}_R]$. Using "Kruskal operator" [17], (1) can be rewritten as

$$\boldsymbol{\mathcal{X}} \approx [\![\mathbf{A}, \mathbf{B}, \mathbf{C}]\!] \equiv \sum_{r=1}^{R} \mathbf{a}_r \circ \mathbf{b}_r \circ \mathbf{c}_r. \tag{2}$$

Problem (2) can be formulated as a least-square optimization problem:

$$\min_{\mathbf{A},\mathbf{B},\mathbf{C}} \quad f \equiv \frac{1}{2} \left\| \boldsymbol{\mathcal{X}} - [\![\mathbf{A}, \mathbf{B}, \mathbf{C}]\!] \right\|^2. \tag{3}$$

Finally, the nonlinear conjugate gradient (NCG) method is employed to solve the optimization problem and consequently find the tensor factors – $\mathbf{A} \in \mathbb{R}^{L\times R}$ and $\mathbf{B} \in \mathbb{R}^{M\times R}$, and $\mathbf{C} \in \mathbb{R}^{N\times R}$ corresponding respectively to the temporal, special, and segmental factors. For more details, the reader is referred to [16].

2.1. Temporal Component Analysis

The morphology of IEDs resembles each other. Therefore, projecting the IED and non-IED segments onto the temporal components can provide discriminative features. In TCA, Khatri-Rao product is employed for projection as follows:

$$\mathbf{Y}_k = \mathbf{A}^T \odot \mathbf{X}_k^T, \tag{4}$$

where the symbol '$\odot$' denotes Khatri-Rao product, $\mathbf{X}_k \in \mathbb{R}^{L\times M}$ is an IED or non-IED segment, and $\mathbf{Y}_k \in \mathbb{R}^{(MR)\times L}$ represents the same segment after projection onto the temporal factors.

2.2. Spatial Component Analysis

It is clear that the IEDs originate from the same location. Thus, by projecting the IED and non-IED segments onto the spatial factors, we can derive the discriminative features. The projection is performed as follows:

$$\bar{\mathbf{Y}}_k = \mathbf{X}_k \mathbf{B} \tag{5}$$

where $\bar{\mathbf{Y}}_k \in \mathbb{R}^{L\times R}$ is the projected IED or non-IED segment onto the spatial factors.

2.3. TCA-SCA

To improve the performance of IED detection system, SCA and TCA are combined. In TCA-SCA, each segment is given separately to SCA and TCA to be classified. Then, those segments that are classified in the IED class by both methods are recognized as the IEDs.

3. EXPERIMENTS

3.1. Data Description

The scalp and intracranial EEGs with a length of 20 minutes were simultaneously recorded from 7 epileptic subjects at King's College Hospital London. Eighteen electrodes were employed according to the 'Maudsley' electrode placement system [18] to record the sEEG, and 12 intracranial multicontact FO electrodes to record the iEEG at the sampling rate

Table 1: The number of all IEDs and scalp-visible IEDs for each subject in the training. The percentage of scalp-visible IEDs from all IEDs is illustrated in parentheses. The same number of non-IED segments were selected for each subject.

Subject	No. of all IEDs	No. of scalp-visible IEDs (their percentage from all IEDs)
S1	182	36 (19.7%)
S2	270	16 (5.9%)
S3	179	3 (1.6%)
S4	482	6 (1.2%)
S5	420	3 (0.7%)
S6	303	0 (0.0%)
S7	135	42 (31.1%)
Mean	—	— (8.5%)

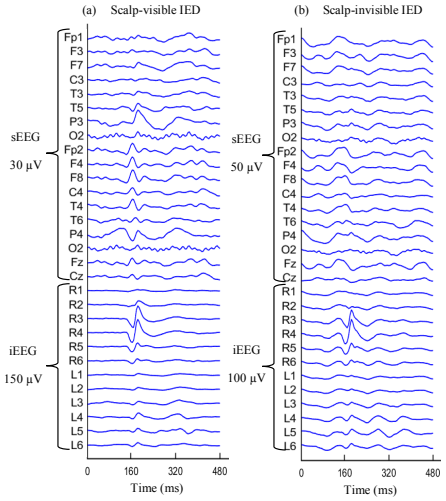

Fig. 2: Samples of (a) scalp-visible and (b) scalp-invisible IEDs. Channels R1 to R6 and L1 to L6 correspond respectively to the FO channels of right and left hemispheres. The IEDs start at 160 ms.

of 200 Hz. A bandpass filter of 4-70 Hz bandwidth and a notch filter with notch frequency of 50 Hz were applied to both sEEG and iEEG signals in order to increase the signal-to-noise ratio and eliminate the power line interference.

3.2. Training and Test Datasets

An expert epileptologist annotated IEDs from the iEEG recordings. The first 10-minute recordings are used as the training data. For training the models, the IED segments were selected from the training signals with a length of 480 ms (96 samples). The peaks marked as the IEDs were centered at between 30^{th} to 34^{th} sample of IED segments. That is, the maximum difference between the IED peaks was 4 samples in the training dataset. Non-IED segments with 480 ms length were selected from the time segments in which there were no scored IEDs. We chose the same number of IED and non-IED segments for each subject to have a balanced classification problem.

The number of all IEDs and scalp-visible IEDs are shown in Table 1. The most scalp-visible IEDs appear in subject 7 with 31.1%. For subjects 3-6, the percentage of scalp-visible IEDs is less than 2. However, their average across subjects is 8.5% in the training dataset. Figure 2 shows samples of scalp-visible and invisible IEDs.

Table 2: The number of all IEDs and scalp-visible IEDs existed in the ongoing test data. The percentage of scalp-visible IEDs from all IEDs is illustrated in parentheses.

Subject	No. of all IEDs	No. of scalp-visible IEDs (their percentage from all IEDs)
S1	160	14 (8.7%)
S2	202	3 (1.4%)
S3	162	17 (10.4%)
S4	366	5 (1.3%)
S5	408	1 (0.2%)
S6	303	0 (0.0%)
S7	89	10 (11.2%)
Mean	—	— (4.7%)

The second 10-minute recordings are used as the test data. A window of 96-sample length and 4-sample stride is slid along the test signals. Because of this 4-sample stride, the IEDs were not centered at the same point in the training dataset. However, after sliding the whole test signals, we have 30000 segments (a few IED segments and numerous non-IED segments) for each subject.

3.3. Training the Models and Detecting IED from Ongoing Signals

The IED segments in the training dataset, shown by N, are concatenated into a three-way tensor $\boldsymbol{\mathcal{X}} \in \mathbb{R}^{96\times M\times N}$, where 96 is time samples and M is the number of recorded channels ($M = 18$ for sEEG and $M = 12$ for iEEG). CPD is employed to decompose the tensor into the temporal, $\mathbf{A} \in \mathbb{R}^{96\times R}$, spatial, $\mathbf{B} \in \mathbb{R}^{M\times R}$, and segmental, $\mathbf{C} \in \mathbb{R}^{N\times R}$, factors.

In TCA, both IED and non-IED segments are projected onto the temporal factors by (4). Then, the magnitudes of short-time Fourier transform are obtained from the projected segments $\mathbf{Y}_k \in \mathbb{R}^{(MR)\times 96}$ using the spectrogram. In the spectrogram, a Hanning window with a length of 80 ms (16 samples) and 50% overlap is applied. The number of discrete Fourier transform points is selected to be 16 resulting in 9 frequency features. Totally, we obtain $(MR)\times 11\times 9$ features (M and R respectively correspond to the number of channels and factors, 11 and 9 are respectively the number of time and frequency features) for each IED or non-IED segment.

In SCA, the segments are projected onto the spatial factors by (5). Then, TF features, as described above, are obtained from the projected segments $\bar{\mathbf{Y}}_k \in \mathbb{R}^{96\times R}$. In this method, $R \times 11 \times 9$ features are extracted.

The optimized number of components R is determined by k-fold nested cross-validation technique. The training dataset is divided into 5 folds. Four folds are employed to train a classifier, and the rest for validation. This procedure is repeated for all folds. We found that CPD with 3 components $(R = 3)$ provides the best performance.

Table 3: The performance of classifiers detecting IEDs from the iEEG. SEN is shown in percent (%). The mean of FP/min is adjusted to be around 5 by choosing a high threshold for the classifier.

Subject	TCA		SCA		TCA-SCA	
	SEN	FP/min	SEN	FP/min	SEN	FP/min
S1	**95.0**	5.7	91.8	3.7	93.7	3.8
S2	54.4	6.5	54.4	5.9	**59.4**	7.1
S3	75.9	6.2	**82.1**	6.7	78.4	6.4
S4	94.0	4.5	94.5	3.5	94.5	3.2
S5	71.3	5.1	75.7	5.9	**80.0**	7.2
S6	74.2	4.7	74.2	4.9	**75.6**	4.9
S7	83.1	3.9	80.9	5.8	**86.5**	4.2
Mean	78.3	5.2	79.1	5.2	**81.2**	5.2

Table 4: The performance of classifiers detecting IEDs from the sEEG. SEN is shown in percent (%). The mean of FP/min is adjusted to be around 5 by choosing a high threshold for the classifier.

Subject	TCA		SCA		TCA-SCA	
	SEN	FP/min	SEN	FP/min	SEN	FP/min
S1	61.2	5.0	49.4	3.0	**64.4**	3.4
S2	27.2	5.6	**35.6**	6.6	25.2	7.1
S3	22.2	6.1	**32.7**	6.7	30.2	5.6
S4	**27.3**	6.4	25.7	7.0	20.0	6.7
S5	**36.2**	4.9	28.2	5.1	32.3	3.9
S6	40.9	7.6	40.9	5.8	**44.9**	7.2
S7	30.3	1.8	29.2	3.7	**44.9**	3.3
Mean	35.1	5.3	34.5	5.4	**37.4**	5.3

Decision tree is employed for classification. The classifier is trained separately for each subject by all training trials. For detecting the IEDs from the ongoing signals, a 96-sample window with 4-sample stride slides along the signals. Each window is given to TCA and SCA to be classified as an IED or non-IED. Recall that TCA-SCA is the combined model of TCA and SCA. If both TCA and SCA detect a segment as an IED, TCA-SCA categorize it in the IED class. Otherwise, the segment is categorized in the non-IED class.

4. RESULTS AND DISCUSSION

For evaluation of the methods, the sensitivity (SEN) and false positive rate per minute (FP/min) are calculated. SEN shows the percentage of IEDs detected correctly, and FP/min is the number of non-IED segments recognized as IEDs incorrectly per minute. In all methods, a high threshold value is selected for the classifier to have the average of around 5 FP/min.

In evaluation procedure, IEDs are not given as a segment to the models. A window slid across the ongoing signals. Therefore, there is no alignment among IED segments, causing to the decrease of sensitivity and increase of FP rate. However, a segment classified as an IED segment counts as true positive if an IED segment exists 32 samples before or after the detected sample, otherwise it counts as FP.

The number of IEDs as well as sclp-visible IEDs for the test signal is shown in Table 2. The average of scalp-visible IEDs is 4.7%, which is extremely low. Around 10% of IEDs are visible over the scalp in subjects 1, 3, and 7, and less than 1.5% in subjects 2 and 4, and approximately 0% in subjects 5 and 6.

Table 3 illustrates the performance of methods in detecting the IEDs from ongoing iEEG recordings. The methods provide different SEN and FP/min values for different subjects. TCA detects IEDs with 78.3% SEN. SCA provides a higher performance of 79.1% SEN. However, TCA-SCA outperforms both TCA and SCA by achieving 81.2% SEN. All three methods detect IEDs with 5.2 FP/min.

The performance of methods in detecting the IEDs from sEEG signals is shown in Table 4. TCA and SCA respectively detect IEDs with 35.1% and 34.5% SEN. However, the best performance is obtained by TCA-SCA providing 37.4% SEN. TCA-SCA detects IEDs of subject 1 with 64.4 SEN. For subjects 6 and 7, it achieves the SEN of 44.9 %. However, the amount of SEN is less than 33% for other subjects.

The IEDs are labeled based on the iEEG. In other words, the iEEG is used as a ground truth for labeling the IEDs. Therefore, a large proportion of IEDs in our data is invisible over the scalp. The percentage of scalp-visible and invisible IEDs in the data used in this study was already analyzed [6]. In their study, the IEDs of 20 patients were used. They showed that only 9% of IEDs averaged across all 20 subjects is visible in their sEEG. These scalp-visible IEDs were observed from 13 out of 20 subjects, meaning that some patients may not have scalp-visible IEDs. In our dataset, 7 patients are examined. In the test data, only 4.7% of IEDs are observable in our sEEG. Even, subject 6 has no scalp-visible IEDs. However, the obtained results from the sEEG show that the proposed method enables detection of scalp-invisible IEDs from the sEEG by fair sensitivity and low FP/min. The obtained SEN from the sEEG is significantly higher than the percentage of scalp-visible IEDs for all subjects.

5. CONCLUSION

In this study, we develop a method based on tensor factorization and temporal component analysis, called TCA, to detect the IEDs from ongoing concurrent sEEG and iEEG recordings. In addition, an already developed method based on spatial component analysis, namely SCA, is employed for IED detection. At the end, the results of TCA and SCA are combined to improve the sensitivity. TCA-SCA outperforms others by providing 81.2% and 37.4% SEN when the IEDs are detected respectively from the iEEG and sEEG. The obtained results are promising since only 4.7% of IEDs are visible from our sEEG dataset. The findings show that the scalp-visible IEDs can be detected from ongoing sEEG recordings by multi-way analysis.

6. REFERENCES

[1] S. Sanei and J. A. Chambers, *EEG Signal Processing and Machine Learning*. John Wiley & Sons, 2021.

[2] H. Wieser, C. Elger, and S. Stodieck, "The 'foramen ovale electrode': a new recording method for the preoperative evaluation of patients suffering from mesio-basal temporal lobe epilepsy," *Electroencephalography and Clinical Neurophysiology*, vol. 61, pp. 314–322, 1985.

[3] I. Karakis, N. Velez-Ruiz, J. S. Pathmanathan, S. A. Sheth, E. N. Eskandar, and A. J. Cole, "Foramen ovale electrodes in the evaluation of epilepsy surgery: conventional and unconventional uses," *Epilepsy & Behavior*, vol. 22, pp. 247–254, 2011.

[4] S. A. Sheth, J. P. Aronson, M. M. Shafi *et al.*, "Utility of foramen ovale electrodes in mesial temporal lobe epilepsy," *Epilepsia*, vol. 55, pp. 713–724, 2014.

[5] M. Sparkes, A. Valentin, and G. Alarcon, "Mechanisms involved in the conduction of anterior temporal epileptiform discharges to the scalp," *Clinical Neurophysiology*, vol. 120, pp. 2063–2070, 2009.

[6] D. Nayak, A. Valentin, G. Alarcon *et al.*, "Characteristics of scalp electrical fields associated with deep medial temporal epileptiform discharges," *Clinical Neurophysiology*, vol. 115, pp. 1423–1435, 2004.

[7] M. Yamazaki, D. M. Tucker, A. Fujimoto *et al.*, "Comparison of dense array EEG with simultaneous intracranial EEG for interictal spike detection and localization," *Epilepsy Research*, vol. 98, pp. 166–173, 2012.

[8] L. Spyrou, D. Martín-Lopez, A. Valentín, G. Alarcón, and S. Sanei, "Detection of intracranial signatures of interictal epileptiform discharges from concurrent scalp EEG," *International Journal of Neural Systems*, vol. 26, p. 1650016, 2016.

[9] A. Antoniades, L. Spyrou, D. Martin-Lopez, A. Valentin, G. Alarcon, S. Sanei, and C. C. Took, "Detection of interictal discharges with convolutional neural networks using discrete ordered multichannel intracranial EEG," *IEEE Transactions on Neural Systems and Rehabilitation Engineering*, vol. 25, pp. 2285–2294, 2017.

[10] A. Antoniades, L. Spyrou, D. Martin-Lopez, A. Valentin, G. Alarcon, S. Sanei, and C. C. Took, "Deep neural architectures for mapping scalp to intracranial EEG," *International Journal of Neural Systems*, vol. 28, p. 1850009, 2018.

[11] B. Abdi-Sargezeh, A. Valentin, G. Alarcon, and S. Sanei, "Incorporating uncertainty in data labeling into detection of brain interictal epileptiform discharges from EEG using weighted optimization," in *2021 IEEE International Conference on Acoustics, Speech and Signal Processing (ICASSP)*, 2021, pp. 1000–1004.

[12] L. Spyrou, S. Kouchaki, and S. Sanei, "Multiview classification and dimensionality reduction of scalp and intracranial EEG data through tensor factorisation," *Journal of Signal Processing Systems*, vol. 90, pp. 273–284, 2018.

[13] S. Yuan, J. Liu, J. Shang, F. Xu, L. Dai, and X. Kong, "Automatic seizure prediction based on modified Stockwell transform and tensor decomposition," in *2020 IEEE International Conference on Bioinformatics and Biomedicine (BIBM)*. IEEE, 2020, pp. 1503–1509.

[14] L. T. Thanh, N. T. A. Dao, N. V. Dung, N. L. Trung, and K. Abed-Meraim, "Multi-channel EEG epileptic spike detection by a new method of tensor decomposition," *Journal of Neural Engineering*, vol. 17, p. 016023, jan 2020.

[15] B. Abdi-Sargezeh, A. Valentin, G. Alarcon, and S. Sanei, "Incorporating uncertainty in data labeling into automatic detection of interictal epileptiform discharges from concurrent scalp-EEG via multi-way analysis," *International Journal of Neural Systems*, p. 2150019, March 2021. [Online]. Available: https://doi.org/10.1142/S0129065721500192

[16] E. Acar, D. M. Dunlavy, and T. G. Kolda, "A scalable optimization approach for fitting canonical tensor decompositions," *Journal of Chemometrics*, vol. 25, pp. 67–86, 2011.

[17] T. G. Kolda, "Multilinear operators for higher-order decompositions." Sandia National Laboratories, Tech. Rep., 2006.

[18] J. F. Torre, G. Alarcon, C. Binnie, and C. Polkey, "Comparison of sphenoidal, foramen ovale and anterior temporal placements for detecting interictal epileptiform discharges in presurgical assessment for temporal lobe epilepsy," *Clinical Neurophysiology*, vol. 110, pp. 895–904, 1999.